Inorganic Chemistry

Article

pubs.acs.org/IC

New Salt-Inclusion Borate, $Li_3Ca_9(BO_3)_7$·2[LiF]: A Promising UV NLO Material with the Coplanar and High Density BO_3 Triangles

Hongwei Yu,[†,‡] Hongping Wu,[†] Shilie Pan,*[,†] Ying Wang,[†,‡] Zhihua Yang,[†] and Xin Su[†]

[†]Xinjiang Technical Institute of Physics & Chemistry, Key Laboratory of Functional Materials and Devices under Special Environments, CAS, Xinjiang Key Laboratory of Electronic Information Materials and Devices, 40-1 South Beijing Road, Urumqi 830011, China

[‡]University of Chinese Academy of Sciences, Beijing 100049, China

Supporting Information

ABSTRACT: Introduction of the coplanar BO_3 triangles in the alkali metal and alkaline-earth metal mixed fluoborate generates a new UV nonlinear optical material $[Li_3Ca_9(BO_3)_7]$·2[LiF] (LCBF), which possesses a moderate SHG response as large as that of the KDP and a wide transparent region with a UV cutoff edge at 230 nm. The first-principle theoretical calculation suggests that LCBF has a relatively large birefringence (0.07; 532 nm). These properties make it a potential UV nonlinear optical material. And interestingly, LCBF is a salt-inclusion borate with the Li−F chains residing in the one-dimensional open framework, which caters to the development of the salt-inclusion compound in borate.

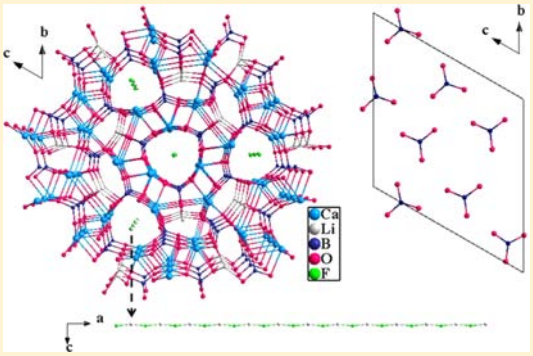

INTRODUCTION

Owing to the prominent properties of ultraviolet (UV) coherent light, such as high photon energy, high spatial resolution, and small heat-affected zone, it has attracted wide attention in microelectronics fabrication, optical data storage, and laser medicine, etc. The best way to produce the UV coherent light with solid-state lasers is to rely on the process of second-harmonic generation (SHG) using nonlinear optical (NLO) materials.[1−11] In order to more effectively realize the frequency conversion, UV NLO materials are required to possess suitable NLO coefficients, a wide transparent region, and a large birefringence for phase-matching. However, it is a big challenge for the UV NLO materials to possess all the above-mentioned properties. For example, we can obtain the large SHG response by involving asymmetric building units in the crystal structure, such as d^0 transition-metal cations (Ti^{4+}, Nb^{5+}, W^{6+}, etc.) susceptible to second-order Jahn−Teller distortion or p cations with stereochemically active lone-pair electrons (Se^{4+}, Te^{4+}, Pb^{2+}, Bi^{3+}, etc).[2,3] But the building units often make the UV absorption edge of the material shift toward the red region, limiting their further applications in the UV region. Therefore, it is of broadly scientific and technological importance to create the subtle balance among the properties NLO materials need.

Over the past decades, borates have been widely considered as ideal candidates for the synthesis of new UV NLO materials because the B−O units, according to the anionic group theory,[4,6] generally are the NLO-active groups and have excitation energies near the UV to favor the wide transparency window.[4−9] Especially when the B−O units are π-delocalization BO_3 triangles or B_3O_6 groups and they adopt the coplanar arrangement, the borates will not only possess large SHG response but also exhibit wide transmission and a large birefringence.[4d,5] Commercial material β-BaB_2O_4 (BBO)[4a] with the anionic B_3O_6 groups exhibits a large SHG response (6 × KDP) and large birefringence (0.12; 532 nm), and $KBe_2BO_3F_2$ (KBBF)[4d] with the coplanar BO_3 triangles exhibits moderate NLO coefficients (1.5 × KDP) and birefringence (0.07; 532 nm). In addition, in our previous work, we combined the coplanar arrangement of BO_3 triangles and the Pb^{2+} cation with the stereoeffect of the lone pair to generate the phase-matching oxyborate, $Pb_4O(BO_3)_2$, which also exhibits the good linear and NLO properties.[7b] However, owing to the introduction of the Pb^{2+} cation, the UV absorption edge of $Pb_4O(BO_3)_2$ shifts toward the red region.

In this study, we retain the coplanar configuration of the BO_3 triangles in the crystal lattices and choose the alkali metal and alkaline-earth metal cations, which have no d−d electron transitions and are ideal for the transmission of UV light. Furthermore, in order to widen the transparency range, the F^- anion is also introduced.[1,7c,11] Thus, a new UV NLO material, $[Li_3Ca_9(BO_3)_7]$·2[LiF] (LCBF), was synthesized. It possesses a moderate SHG response, a wide transparency range, and relatively large birefringence. And interestingly, it contains a channel along the *a* axis, where the Li−F chain resides. So it can be regarded as a LiF salt-inclusion borate.[12] The salt-inclusion solids are common in the compounds containing transition

Received: February 5, 2013
Published: April 12, 2013

   dx.doi.org/10.1021/ic4002779 | Inorg. Chem. 2013, 52, 5359−5365

metal oxide (MO_n, n = 4−6) and oxyanion ($M'O_4^{m-}$, M′ = Si, P, As, Ge) units, in which the salt lattice plays an essential role in bulk structural and chemical/physical properties.[13−15] However, there are relatively few salt-inclusion solids reported in borates.[12c] Therefore, LCBF may serve as the development of the salt-inclusion compound in borates.

2. EXPERIMENTAL SECTION

Reagents. Li_2CO_3 (Tianjin YaoHua Chemical Reagent Co., Ltd., 99.0%), LiF (Tianjin HongYan Chemical Reagent Co., Ltd., 99.0%), CaO (Tianjin Bodi Chemical Co., Ltd., 99.0%), and H_3BO_3 (Tianjin HongYan Chemical Co., Ltd., 99.5%) are used as received.

Crystal Growth. Single crystals of LCBF were grown from the high temperature solution using LiF as the self-flux. The solution was prepared in a platinum crucible by melting a mixture of Li_2CO_3, LiF, CaO, and H_3BO_3 at a molar ratio of 1.5:22:9:7. The platinum crucible was placed in the center of a vertical, programmable temperature furnace, gradually heated to 850 °C, held at this temperature for 20 h, and then cooled to 750 °C. Then, a platinum wire was promptly dipped into the solution. The temperature was lowered to 650 °C at a rate of 2 °C/h. Then, the platinum wire was pulled out of the solution and allowed to cool to room temperature at a rate of 10 °C/h. Thus, some colorless, transparent needlelike crystals were obtained for the structure determination (Figure S1 in the Supporting Information).

X-Ray Crystallographic Studies. The single crystal of LCBF with dimensions 0.12 mm × 0.09 mm × 0.03 mm was selected for the structure determination. The crystal structure of LCBF was determined by single-crystal X-ray diffraction on an APEX II CCD diffractometer using monochromatic Mo Kα radiation (λ = 0.71073 Å) at 296(2) K and intergrated with the SAINT program.[16] Numerical absorption corrections were carried out using the SCALE program for the area detector.[16] All calculations were performed with programs from the SHELXTL crystallographic software package.[17] All atoms were refined using full matrix least-squares techniques; final least-squares refinement is on F_o^2 with data having $F_o^2 \geq 2\sigma(F_o^2)$. The final difference Fourier synthesis map showed the maximum and minimum peaks at 0.451 and −0.446 e·Å^{-3}, respectively. The structure was checked with PLATON,[18] and no higher symmetries were found. Crystal data and structure refinement information are given in Table 1. The final refined atomic positions and isotropic thermal parameters are summarized in Table 2. Selected bond lengths and angles (deg) for LCBF are listed in Table S1 in the Supporting Information.

Compound Synthesis. A polycrystalline sample of LCBF is prepared with solid-state reaction techniques. A stoichiometric mixture of Li_2CO_3 (0.015 mol), LiF (0.02 mol), CaO (0.09 mol), and H_3BO_3 (0.07 mol) was ground and loaded into a platinum crucible. The mixture was preheated at 300 °C for 4 h. Then the temperature was raised to 550 °C and held at that temperature for 48 h with several intermediate grindings and mixings.

X-ray powder diffraction analysis of LCBF is performed at room temperature in the angular range of 2θ = 10∼70° with a scan step width of 0.02° and a fixed counting time of 1 s/step using a Bruker D2 PHASER diffractometer equipped with a diffracted beam monochromator set for Cu Kα radiation (λ = 1.5418 Å). The experimental X-ray powder diffraction pattern is in agreement with the calculated one based on the single-crystal crystallographic data of LCBF (Figure S2 in the Supporting Information).

Infrared Spectroscopy. The infrared spectrum in the 400−4000 cm^{-1} range was recorded on Shimadzu IR Affinity-1 Fourier transform infrared spectrometer in order to specify the coordination of boron in LCBF. The sample was mixed thoroughly with dried KBr, and the characteristic absorption peaks are shown in Figure 2.

UV−Vis−NIR Diffuse Reflectance Spectrum. The optical diffuse reflectance spectrum was measured at room temperature with a Shimadzu SolidSpec-3700DUV spectrophotometer. Data were collected in the wavelength range 200−2500 nm. And the reflectance spectrum was converted to absorbance with the Kubelka−Munk function.[19,20]

Table 1. Crystal Data and Structure Refinement for LCBF

empirical formula	$Li_5Ca_9(BO_3)_7F_2$
formula weight	845.09
temperature	296(2) K
wavelength	0.71073 Å
crystal system	triclinic
space group, Z	$P1$, 1
unit cell dimensions	a = 3.5631(6) Å
	b = 12.872(3) Å
	c = 12.876(2) Å
	α = 60.098(11)°
	β = 88.407(12)°
	γ = 88.420(13)°
volume	511.69(16) Å^3
density (calculated)	2.743 Mg/m^3
absorption coefficient	2.434/mm
F(000)	416
crystal size	0.124 mm × 0.086 mm × 0.033 mm
θ range for data collection	1.82° to 27.56°
limiting indices	$-4 \leq h \leq 4$, $-16 \leq k \leq 16$, $-16 \leq l \leq 16$
reflections collected/ unique	8575/4174 [R(int) = 0.0340]
completeness to θ = 27.56	98.9%
refinement method	full-matrix least-squares on F^2
goodness-of-fit on F^2	1.029
final R indices [$F_o^2 > 2\sigma(F_o^2)$][a]	R_1 = 0.0335, wR_2 = 0.0667
R indices (all data)[a]	R_1 = 0.0392, wR_2 = 0.0705
extinction coefficient	0.0012(9)
largest diff. peak and hole	0.451 and −0.446 e·Å^{-3}

[a] $R_1 = \sum||F_o| - |F_c||/\sum|F_o|$ and $wR_2 = [\sum w(F_o^2 - F_c^2)^2/\sum wF_o^4]^{1/2}$ for $F_o^2 > 2\sigma(F_o^2)$.

Thermal Analysis. Thermal gravimetric (TG) and differential scanning calorimetry (DSC) were investigated with a simultaneous NETZSCH STA 449C thermal analyzer instrument in an atmosphere of flowing N_2. The sample heated from 50 to 1300 °C at a rate of 10 °C/min.

Second-Order NLO Measurements. The SHG test was performed on the powder sample of LCBF using the Kurtz−Perry method.[21] The polycrystalline LCBF was ground and sieved into distinct particle size ranges, <20, 20−38, 38−55, 55−88, 88−105, 105−150, and 150−200 μm, and the microcrystalline KDP was also served as a reference. The sample was then placed in a 0.2-mm-thick quartz cell and irradiated with a Q-switched Nd:YAG solid-state laser (1064 nm, 10 kHz, 10 ns). The intensity of the frequency-doubled output emitted from the sample was measured using a photomultiplier tube.

Numerical Calculation Details. Our calculations employed the CASTEP module as implemented in Materials Studio 5.5. The total plane-wave pseudopotential method forms the basis of the CASTEP calculations.[22] The exchange−correlation effects were treated within the general gradient approximation (GGA) using the Perdew−Burke−Emzerhoff (PBE) functional.[23] The following orbital electrons were treated as valence electrons: Li, $1s^22s^1$; F, $2s^22p^5$; B, $2s^22p^1$; Ca, $3s^23p^64s^2$; O, $2s^22p^4$. The plane-wave basis set energy cutoff was set at 540.0 eV; ultrasoft pseudopotentials were used for all chemical elements. The Monkhorst−Pack scheme k-point grid sampling was set at 4 × 4 × 4 for the Brillouin zone. The convergence parameters were as follows: total energy tolerance 2 × 10^{-6} eV/atom.

3. RESULTS AND DISCUSSION

Crystal Structure. LCBF crystallizes in space group $P1$ (no. 1) of the triclinic system. In the asymmetric unit, there are five unique Li atoms, nine unique Ca atoms, seven unique B atoms,

dx.doi.org/10.1021/ic4002779 | Inorg. Chem. 2013, 52, 5359−5365

Table 2. Atomic Coordinates (×10^4) and Equivalent Isotropic Displacement Parameters (Å^2 × 10^3) for LCBF[a]

atom	x	y	z	U(eq)	BVS
Ca(1)	550(3)	2403(1)	6131(1)	13(1)	2.111
Ca(2)	837(3)	4863(1)	2189(1)	12(1)	2.185
Ca(3)	−4268(3)	54(1)	5894(1)	12(1)	2.203
Ca(4)	5585(3)	7464(1)	−172(1)	12(1)	2.158
Ca(5)	10407(3)	6359(1)	4704(1)	13(1)	2.140
Ca(6)	5455(3)	6112(1)	7305(1)	13(1)	2.149
Ca(7)	−3700(2)	2735(1)	1578(1)	11(1)	1.969
Ca(8)	5351(3)	1801(1)	8877(1)	14(1)	1.872
Ca(9)	15132(3)	9075(1)	2555(1)	13(1)	1.972
Li(1)	10300(20)	9082(8)	444(8)	15(2)	0.942
Li(2)	−9010(30)	620(9)	3667(8)	20(2)	0.961
Li(3)	10470(20)	3861(8)	8929(8)	17(2)	0.995
Li(4)	5660(40)	4690(20)	4200(20)	91(6)	0.796
Li(5)	10550(40)	8070(19)	−2444(19)	111(9)	0.790
B(1)	526(16)	−23(6)	8151(5)	10(1)	3.014
B(2)	456(16)	8343(6)	5116(6)	9(1)	3.022
B(3)	753(15)	5285(6)	−204(5)	9(1)	2.968
B(4)	5456(16)	7068(6)	2223(6)	13(1)	3.020
B(5)	577(15)	1173(5)	1018(5)	12(1)	3.140
B(6)	5384(15)	4116(5)	6895(6)	11(1)	3.044
B(7)	−4094(15)	2383(5)	3923(5)	11(1)	3.009
O(1)	−3849(10)	1409(3)	3764(3)	15(1)	1.946
O(2)	5319(10)	3965(3)	8038(3)	16(1)	1.823
O(3)	15333(10)	8201(3)	1236(3)	14(1)	1.905
O(4)	5456(9)	6948(3)	3346(3)	13(1)	2.016
O(5)	5409(9)	3134(3)	6758(3)	14(1)	2.083
O(6)	−4372(10)	2223(3)	5064(3)	13(1)	1.998
O(7)	5694(10)	6085(3)	2073(3)	12(1)	2.052
O(8)	−4091(9)	3522(3)	2925(3)	14(1)	2.028
O(9)	5453(10)	5267(3)	5926(3)	13(1)	1.977
O(10)	1227(9)	4102(3)	712(3)	13(1)	1.901
O(11)	477(9)	7172(3)	6023(3)	14(1)	2.024
O(12)	475(9)	913(3)	8397(3)	15(1)	1.840
O(13)	610(9)	245(3)	6977(3)	14(1)	1.996
O(14)	−9087(9)	−739(3)	5358(3)	13(1)	2.092
O(15)	10096(9)	8596(3)	3941(3)	15(1)	1.890
O(16)	10471(9)	8813(3)	−932(3)	13(1)	2.020
O(17)	715(9)	6186(3)	69(3)	14(1)	2.063
O(18)	20035(9)	10060(3)	1165(3)	16(1)	1.989
O(19)	9876(10)	2168(3)	9956(3)	18(1)	1.991
O(20)	−8155(9)	1278(3)	1963(3)	17(1)	1.979
O(21)	10372(9)	5521(3)	8633(3)	15(1)	2.000
F(1)	600(8)	4545(3)	4342(3)	16(1)	1.018
F(2)	5599(8)	7888(3)	−2319(3)	16(1)	1.049

[a] U_{eq} is defined as one-third of the trace of the orthogonalized U_{ij} tensor.

21 unique O atoms, and two F atoms (Table 2). The Li atoms have two kinds of coordinated environments: Li(1), Li(2), and Li(3) atoms are coordinated by the four O atoms. The Li(4) and Li(5) atoms are coordinated by the two F atoms. The Ca atoms have three kinds of coordinated environments: Ca(1) to Ca(6) are coordinated by the six O atoms and one F atom, respectively, Ca(7) and Ca(9) are coordinated by seven O atoms, and Ca(8) is coordinated to a distorted octahedron of six O atoms. And all the B atoms are the planar BO_3 triangles.

The structure of LCBF is illustrated in Figure 1. The Li-centered polyhedra, the Ca-centered polyhedra, and the isolated BO_3 triangles connect with each other via vertex-sharing or edge-sharing to form a complicated three-dimensional (3D) network with a channel along the *a* axis, where the one-dimensional Li−F chains are filled (Figure 1a). And the Li−F chains are weakly fixed in the channel by the relatively longer Ca−F bonds, due to their electronegativity difference.[24] The average bond length of the Ca−F bonds is 2.573 Å, which is longer than 2.36 Å, the sum of Shannon crystal radii of 7-coordinated Ca^{2+} (1.2 Å) and 3-coordinated F^- (1.16 Å).[25] The weak interaction between the Li−F chains and $Li_3Ca_9(BO_3)_7$ framework demonstrates that LCBF can be seen as a salt-inclusion borate with a structural formula of $[Li_3Ca_9(BO_3)_7]\cdot 2[LiF]$. And the channel of $Li_3Ca_9(BO_3)_7$ framework is 5.9 Å in diameter, which may be large enough to allow a chemical modification via ion-exchange reactions.

In addition, it is particularly worth noting that, in the crystal structure of LCBF, all the B−O groups are isolated BO_3

dx.doi.org/10.1021/ic4002779 | Inorg. Chem. 2013, 52, 5359−5365

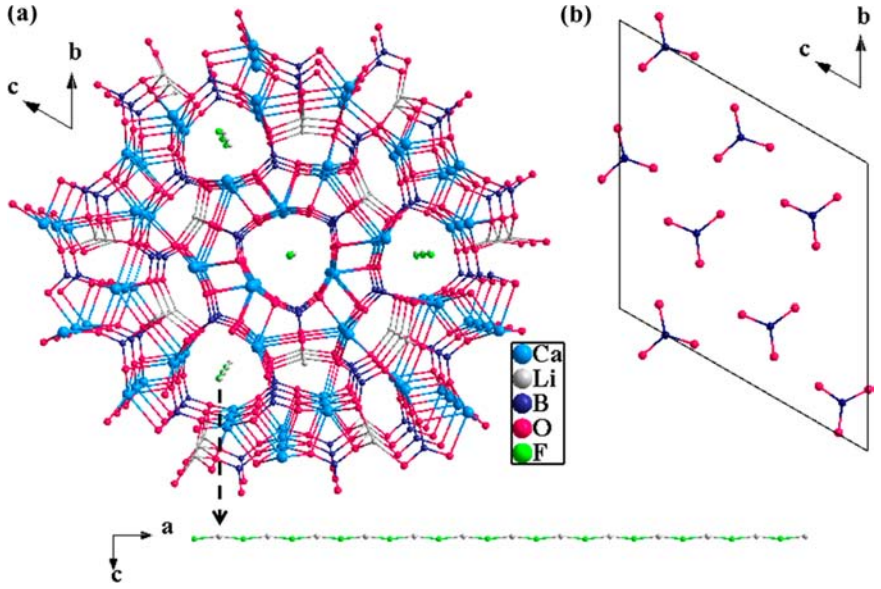

Figure 1. (a) The one-dimensional open-framework structure filled with the Li−F chain (Li−O bonds omitted for clarity). (b) The coplanar arrangement of BO_3 triangles in the unit cell.

triangles. The isolated BO_3 triangles adopt almost coplanar configuration (Figure 1b) and have a high number density (0.0137 $Å^{-3}$), which is higher than that in KBBF[1] (0.0094 $Å^{-3}$) and is comparable to that in $Sr_2Be_2B_2O_7$[6a] (0.0137 $Å^{-3}$). The high density and coplanar arrangement of BO_3 triangles will be favorable for LCBF to exhibit relatively large SHG response and birefringence, which has been highlighted before.[26]

In the structure of LCBF, the Ca−O bond lengths have a wide region varying from 2.309(3) to 2.800(4) Å, and Ca−F bond lengths vary from 2.538(3) to 2.598(3) Å. The Li−O bond lengths and Li−F bond lengths vary from 1.901(9) to 2.161(10) Å and 1.772(15) to 1.811(15) Å, respectively. The B−O bond lengths range from 1.352(7) to 1.395(7) Å. All of the bond lengths are consistent with those observed in other compounds.[27−29] The results of bond valence calculations (Li, 0.79−0.995; Ca, 1.87−2.20; B, 2.97−3.14; F, 1.018−1.049) indicate that the Li, Ca, B, and F atoms are in oxidation states of +1, +2, +3, and −1, respectively.[30,31]

IR Measurement. As shown in Figure 2, the strong broad band around 1300 cm^{-1} in the curve is attributed to the BO_3 asymmetric and symmetric stretching vibrations. The bands at 769, 736, 651, and 518 cm^{-1} can be characteristics of BO_3 bending vibration. It is in agreement with other compounds containing the BO_3 group.[32−34]

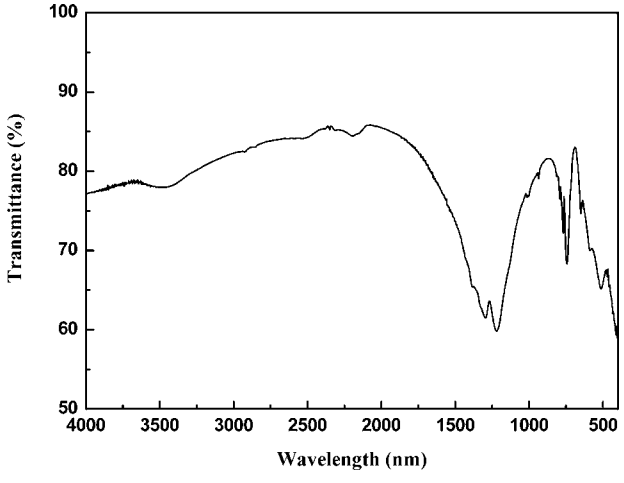

Figure 2. IR spectrum of LCBF.

The UV−Vis−NIR Diffuse Reflectance Spectrum. UV−Vis−NIR diffuse reflectance spectrum of LCBF is shown in Figure 3. It has a cutoff edge of about 230 nm, indicating that the crystal may have potential use in UV NLO applications.

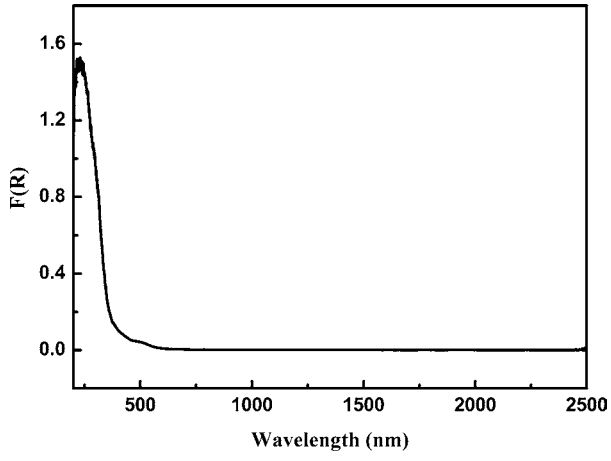

Figure 3. UV−vis−NIR diffuse reflectance spectrum of LCBF.

Thermal Analysis. The TG/DSC curves of LCBF are shown in Figure S3 in the Supporting Information. On the DSC curve, one strong endothermic peak at 656 °C, following some weak endothermic peaks, is observed. And there is no weight loss observed on the TG curve before 900 °C. Those indicate that LCBF is stable until 656 °C. Furthermore, in order to understand the effect at 656 °C, we calcined the pure LCBF powders at this temperature with different reaction times. The powder X-ray diffraction patterns were measured on each obtained sample, and the results are shown in Figure S2 in the Supporting Information. When the reaction time is 2 h, the samples mainly contain two phases, LCBF and $Ca_3(BO_3)_2$

dx.doi.org/10.1021/ic4002779 | Inorg. Chem. 2013, 52, 5359−5365

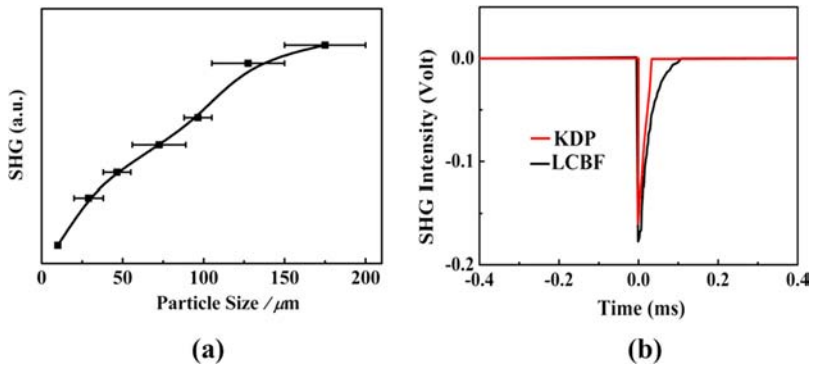

Figure 4. (a) Phase-matching, that is, particle size vs SHG intensity, data for LCBF. The solid curve drawn is to guide the eye and is not a fit to the data. (b) SHG intensities of LCBF with commercial KDP as a reference: Oscilloscope traces for the powder of KDP and LCBF.

(ICDD PDF No. 73-1203). However, when the reaction time is 20 h, the samples almost decompose into $Ca_3(BO_3)_2$ (ICDD PDF No. 73-1203) and an unknown phase. Therefore, the endothermic peak at 656 °C is due to the decomposition of LCBF, and the following weak peaks may correspond to the melting of the unknown phase. In addition, it should also be noted that there is an obvious weight loss accompanying the continuous endothermic effect at a higher temperature than 900 °C, which may be caused by the volatilization of fluoride and B_2O_3.

Nonlinear Optical Properties. The plot of the second-harmonic intensity vs particle size of the LCBF powders is shown in Figure 4. It is clear that the second-harmonic intensity becomes larger with the particle size of the LCBF powders increasing (Figure 4a). It is consistent with phase-matching behavior according to the rule proposed by Kurtz and Perry.[21] And when a KDP sample with the same size was used as a reference, it was found that LCBF has a powder SHG effect as large as that of KDP (Figure 4b).

According to the anionic-group theory,[4,6] the SHG response of borate NLO materials mainly originates from the B−O units. That is to say, the number density and overall arrangement of the B−O units will determine the SHG response. As described in the Crystal Structure section, in LCBF, all the B−O groups are the BO_3 triangles and adopt a coplanar arrangement in (001). However, the coplanar arrangement of BO_3 triangles is not totally in the same orientation. In order to better quantify the orientation of the BO_3 triangles, we calculated the dipole moment of the BO_3 triangles using a simple bond-valence approach.[35] It is found that all the total net dipole moment in the unit cell generated by the BO_3 triangles is 1.196 D, which is 41.3% of its optimal value, 2.898 D (all the BO_3 triangles have the same orientation; Table 3). It suggests that over half of the microscopic SHG response generated by BO_3 triangles is canceled in LCBF. However, the number density (0.0137 $Å^{-3}$) of BO_3 triangles makes LCBF preserve a moderate SHG response, as large as that of KDP.

Electronic Structure. Since the optical properties in the visible and UV spectrum are mainly determined by the states close to the band gap,[36] only the upper region of the valence band (VB) and the bottom of the conduction band (CB) are shown in Figure 5. Clearly, LCBF is a direct gap compound, and the gap is 4.33 eV at G point (Figure 5a). The upper region of VB is mainly derived from O 2p with a tiny contribution of Li 2p and F 2p states, and the bottom of CB is mainly composed of B 2p states mixing with a small amount of B 2s and Li 2p states (Figure 5b). That indicates that the optical properties of LCBF primarily come from BO_3 groups.

Table 3. The Dipole Moments of the BO_3 Triangles in the Unit Cell

species		*x*	*y*	*z*	Debye
$B(1)O_3$		−0.0550	0.4404	−0.1400	0.3959
$B(2)O_3$		0.4400	−0.0515	−0.2556	0.5223
$B(3)O_3$		0.2057	−0.3474	0.2454	0.3791
$B(4)O_3$		0.4058	0.3849	−0.1477	0.5174
$B(5)O_3$		0.0450	−0.2267	0.3635	0.3233
$B(6)O_3$		0.1261	0.0566	0.5075	0.5537
$B(7)O_3$		−0.1120	−0.0404	−0.1485	0.2060
unit cell	experimental	1.0556	0.2160	0.4246	1.1969
	optimal value[b]				2.8978

[b]The optimal value of the dipole moment in the unit cell is calculated by $\sum_{i=1}^{7}\mathbf{B}(i)\mathbf{O}_3$.

Optical Property. On the basis of the electronic structure, the dispersions of the linear refractive indices are calculated. The birefringence in the visible region is displayed in Figure 6. LCBF is a negative biaxial crystal and has a relatively large birefringence (0.07; 532 nm), which is mainly derived from the coplanar arrangement of BO_3 triangles in LCBF. Furthermore, LCBF has 10 independent SHG coefficients under the restriction of Kleinman symmetry, and our ab initio calculations reveal that the largest SHG coefficient d_{33} is 0.58 pm/V, about 1.4 times that of KDP (0.39 pm/V), which is consistent with the experimental results.

CONCLUSION

A new UV NLO material, LCBF, was reported. Structurally, it is the salt-inclusion borate with Li−F chains filling in the channel of the $Li_3Ca_9(BO_3)_7$ framework. And more importantly, in its crystal structure, all the BO_3 units adopt coplanar arrangement and have a high number density. The high number density and coplanar arrangement of BO_3 triangles make LCBF possess a moderate SHG response and a relatively large birefringence. And since the alkali metal and alkaline-earth metal cations have no d−d electron transitions, LCBF shows a wide transparent region with a UV cutoff edge at about 230 nm. The moderate SHG response and large birefringence, as well as the wide transparent region, will be favorable for the practical applications of LCBF as a UV NLO material. Our future efforts will be devoted to the growth of large crystals and relevant physical properties studies for this compound.

dx.doi.org/10.1021/ic4002779 | Inorg. Chem. 2013, 52, 5359−5365

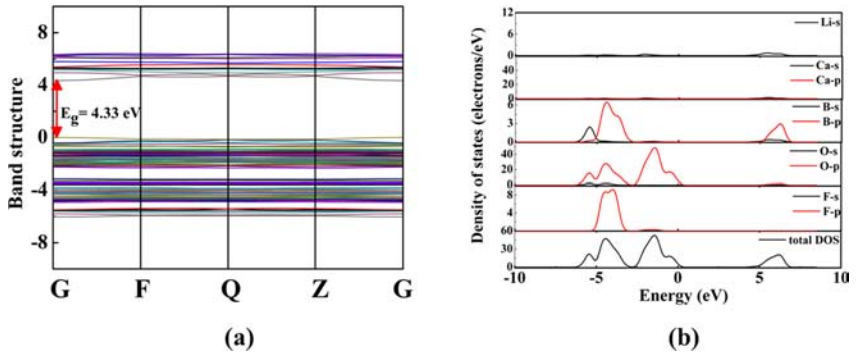

Figure 5. (a) Calculated band structure of LCBF. (b) The densities of states of LCBF.

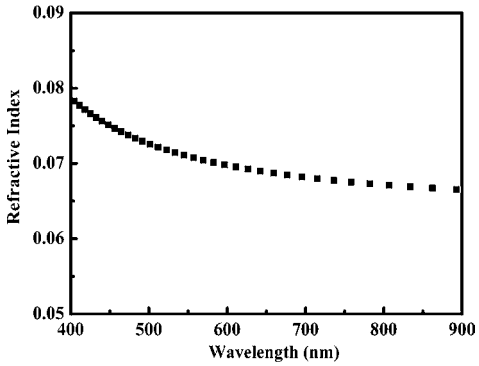

Figure 6. The calculated birefringence of LCBF in the visible region.

■ ASSOCIATED CONTENT

Supporting Information

Selected bond lengths and angles, a photograph of as-grown LCBF crystals, a comparison of the experimental and calculated powder X-ray diffraction patterns and the powder X-ray diffraction patterns at 656 °C with different reaction times, and TG/DSC curves of LCBF. This material is available free of charge via the Internet at http://pubs.acs.org.

■ AUTHOR INFORMATION

Corresponding Author

*E-mail: slpan@ms.xjb.ac.cn (Shilie Pan).

Notes

The authors declare no competing financial interest.

■ ACKNOWLEDGMENTS

This work is supported by the National Key Basic Research Program of China (Grant No. 2012CB626803), the "National Natural Science Foundation of China" (Grant Nos. U1129301, 51172277, 21101168, 11104344, 21201176), Main Direction Program of Knowledge Innovation of Chinese Academy of Sciences (Grant No. KJCX2-EW-H03-03), the "One Hundred Talents Project Foundation Program" of Chinese Academy of Sciences, Major Program of Xinjiang Uygur Autonomous Region of China during the 12th Five-Year Plan Period (Grant No. 201130111), the "High Technology Research and Development Program" of Xinjiang Uygur Autonomous Region of China (Grant No. 201116143).

■ REFERENCES

(1) Becker, P. *Adv. Mater.* **1998**, *10*, 979.
(2) (a) Ra, H. S.; Ok, K. M.; Halasyamani, P. S. *J. Am. Chem. Soc.* **2003**, *125*, 7764. (b) Inaguma, Y.; Yoshida, M.; Katsumata, T. *J. Am. Chem. Soc.* **2008**, *130*, 6704. (c) Yang, B. P.; Hu, C. L.; Xu, X.; Sun, C. F.; Zhang, J. H.; Mao, J. G. *Chem. Mater.* **2010**, *22*, 1545. (d) Donakowski, M. D.; Gautier, R.; Yeon, J.; Moore, D. T.; Nino, J. C.; Halasyamani, P. S.; Poeppelmeier, K. R. *J. Am. Chem. Soc.* **2012**, *134*, 7679.
(3) (a) Chang, H. Y.; Kim, S. H.; Halasyamani, P. S.; Ok, K. M. *J. Am. Chem. Soc.* **2009**, *131*, 2426. (b) Sun, C. F.; Hu, C. L.; Mao, J. G. *Chem. Commun.* **2012**, *48*, 4220. (c) Huang, Y. Z.; Wu, L. M.; Wu, X. T.; Li, L. H.; Chen, L.; Zhang, Y. F. *J. Am. Chem. Soc.* **2010**, *132*, 12788. (d) Zhang, W. L.; Cheng, W. D.; Zhang, H.; Geng, L.; Lin, C. S.; He, Z. Z. *J. Am. Chem. Soc.* **2010**, *132*, 1508. (e) Li, F.; Hou, X. L.; Pan, S. L.; Wang, X. *Chem. Mater.* **2009**, *21*, 2846.
(4) (a) Chen, C. T.; Wu, B. C.; Jiang, A. D.; You, G. M. *Sci. Sin., Ser. B (Engl. Ed.)* **1985**, *28*, 235. (b) Chen, C. T.; Wu, Y. C.; Jiang, A. D.; You, G. M.; Li, R. K.; Lin, S. J. *J. Opt. Soc. Am. B* **1989**, *6*, 616. (c) Wu, Y. C.; Sasaki, T.; Nakai, S.; Yokotani, A.; Tang, H.; Chen, C. T. *Appl. Phys. Lett.* **1993**, *62*, 2614. (d) Chen, C. T.; Lu, J. H.; Togashi, T.; Suganuma, T.; Sekikawa, T.; Watanabe, S.; Xu, Z. Y.; Wang, J. Y. *Opt. Lett.* **2002**, *27*, 637. (e) Yap, Y. K.; Inagaki, M.; Nakajima, S.; Mori, Y.; Sasaki, T. *Opt. Lett.* **1996**, *21*, 1348.
(5) (a) Sasaki, T.; Mori, Y.; Yoshimura, M.; Yap, Y. K.; Kamimura, T. *Mater. Sci. Eng.* **2000**, *30*, 1. (b) Mori, Y.; Yap, Y. K.; Kamimura, T.; Yoshimura, M.; Sasaki, T. *Opt. Mater.* **2002**, *19*, 1. (c) Hu, Z. G.; Yoshimura, M.; Mori, Y.; Sasaki, T. *J. Cryst. Growth* **2004**, *260*, 287. (d) Hu, Z. G.; Yoshimura, M.; Mori, Y.; Sasaki, T. *J. Cryst. Growth* **2005**, *275*, 232.
(6) (a) Chen, C. T.; Wang, Y. B.; Wu, B. C.; Wu, K. C.; Zeng, W. L.; Yu, L. H. *Nature* **1995**, *373*, 322. (b) Ye, N.; Zeng, W. R.; Wu, B. C.; Huang, X. Y.; Chen, C. T. *Z. Kristallogr.* **1998**, *213*, 452. (c) Hu, Z. G.; Yoshimura, M.; Muramatsu, K.; Mori, Y.; Sasaki, T. *Jpn. J. Appl. Phys.* **2002**, *41*, L1131. (d) Xu, K.; Loiseau, P.; Aka, G.; Maillard, R.; Maillard, A.; Taira, T. *Opt. Express* **2008**, *16*, 17735.
(7) (a) Wu, H. P.; Pan, S. L.; Poeppelmeier, K. R.; Li, H. Y.; Jia, D. Z.; Chen, Z. H.; Fan, X. Y.; Yang, Y.; Rondinelli, J. M.; Luo, H. S. *J. Am. Chem. Soc.* **2011**, *133*, 7786. (b) Yu, H. W.; Pan, S. L.; Wu, H. P.; Zhao, W. W.; Zhang, F. F.; Li, H. Y.; Yang, Z. H. *J. Mater. Chem.* **2012**, *22*, 2105. (c) Yu, H. W.; Wu, H. P.; Pan, S. L.; Yang, Z. H.; Su, X.; Zhang, F. F. *J. Mater. Chem.* **2012**, *22*, 9665. (d) Pan, S. L.; Wu, Y. C.; Fu, P. Z.; Zhang, G. C.; Li, Z. H.; Du, C. X.; Chen, C. T. *Chem. Mater.* **2003**, *15*, 2218. (e) Wang, L.; Pan, S. L.; Chang, L. X.; Hu, J. Y.; Yu, H. W. *Inorg. Chem.* **2012**, *51*, 1852.
(8) (a) Keszler, D. A. *Curr. Opin. Solid State Mater. Sci.* **1996**, *1*, 204. (b) Becker, P.; Bohaty, L.; Frohlich, R. *Acta Crystallogr., Sect. C* **1995**, *51*, 1721.
(9) (a) Yang, Y.; Pan, S. L.; Hou, X. L.; Wang, C.; Poeppelmeier, K. R.; Chen, Z. H.; Wu, H. P.; Zhou, Z. X. *J. Mater. Chem.* **2011**, *21*, 2890. (b) Yang, Y.; Pan, S. L.; Li, H. L.; Han, J.; Chen, Z. H.; Zhao, W. W.; Zhou, Z. X. *Inorg. Chem.* **2011**, *50*, 2415. (c) Huang, H. W.; Yao, J. Y.; Lin, Z. S.; Wang, X.; He, R.; Yao, W.; Zhai, N.; Chen, C. T. *Angew. Chem., Int. Ed.* **2011**, *50*, 9141.
(10) (a) Hagerman, M. E.; Poeppelmeier, K. R. *Chem. Mater.* **1995**, *7*, 602. (b) Maggard, P. A.; Stern, C. L.; Poepplemeier, K. R. *J. Am. Chem. Soc.* **2001**, *123*, 7742. (c) Pan, S. L.; Smit, J. P.; Watkins, B.;

Marvel, M. R.; Stern, C. L.; Poeppelmeier, K. R. *J. Am. Chem. Soc.* **2006**, *128*, 11631. (d) Halasyamani, P. S.; Poeppelmeier, K. R. *Inorg. Chem.* **2008**, *47*, 8427.
(11) (a) Bekker, T. B.; Fedorov, P. P.; Kokh, A. E. *Cryst. Growth Des.* **2011**, *12*, 129. (b) Rashchenko, S. V.; Bekker, T. B.; Bakakin, V. V.; Seryotkin, Y. V.; Shevchenko, V. S.; Kokh, A. E.; Stonoga, S. Y. *Cryst. Growth Des.* **2012**, *12*, 2955. (c) Bekker, T.; Kokh, A.; Fedorov, P. *CrystEngComm* **2011**, *13*, 3822.
(12) (a) West, J. P.; Hwu, S. J. *J. Solid State Chem.* **2012**, *195*, 101. (b) Hwu, S. J.; Ulutagay-Kartin, M.; Clayhold, J. A.; Mackay, R.; Wardojo, T. A.; O'Connor, C. J.; Krawiec, M. *J. Am. Chem. Soc.* **2002**, *124*, 12404. (c) Li, R. K.; Yu, Y. *Inorg. Chem.* **2006**, *45*, 6840.
(13) Etheredge, K. M. S.; Hwu, S.-J. *Inorg. Chem.* **1995**, *34*, 3123.
(14) Huang, Q.; Hwu, S.-J. *Inorg. Chem.* **2003**, *42*, 655.
(15) Mo, X.; Ferguson, E.; Hwu, S.-J. *Inorg. Chem.* **2005**, *44*, 3121.
(16) *SAINT*, version 7.60A; Bruker Analytical X-ray Instruments, Inc.: Madison, WI, 2008.
(17) Sheldrick, G. M. *SHELXTL*, version 6.14; Bruker Analytical X-ray Instruments, Inc.: Madison, WI, 2003.
(18) Spek, A. L. *J. Appl. Crystallogr.* **2003**, *36*, 7.
(19) Kubelka, P.; Munk, F. Z. *Tech. Phys.* **1931**, *12*, 593.
(20) Tauc, J. *Mater. Res. Bull.* **1970**, *5*, 721.
(21) Kurtz, S. K.; Perry, T. T. *J. Appl. Phys.* **1968**, *39*, 3798.
(22) Clark, S. J.; Segall, M. D.; Pickard, C. J.; Hasnip, P. J.; Probert, M. J.; Rrfson, K.; Payne, M. C. *Z. Kristallogr.* **2005**, *220*, 568.
(23) (a) Ceperley, D. M.; Alder, B. J. *Phys. Rev. Lett.* **1980**, *45*, 566. (b) Perdew, J. P.; Zunger, A. *Phys. Rev. B* **1981**, *23*, 5048.
(24) (a) Li, K. Y.; Xue, D. F. *J. Phys. Chem. A* **2006**, *110*, 11332. (b) Li, K. Y; Wang, X.; Xue, D. F. *J. Phys. Chem. A* **2008**, *112*, 7894.
(25) Shannon, R. *Acta Crystallogr., Sect. A* **1976**, *32*, 751.
(26) (a) Xue, D. F.; Zhang, S. *Appl. Phys. A: Mater. Sci. Process.* **1999**, *68*, 57. (b) Xue, D. F.; Betzler, K.; Hesse, H.; Lammers, D. *Solid State Commun.* **2000**, *114*, 21.
(27) Shi, Y. J.; Wang, Y.; Pan, S. L.; Yang, Z. H.; Dong, X. Y.; Wu, H. P.; Zhang, M.; Cao, J.; Zhou, Z. X. *J. Solid State Chem.* **2013**, *197*, 128.
(28) Luo, J.; Pan, S. L.; Li, H. Y.; Zhou, Z. X.; Yang, Z. H. *J. Mater. Sci.* **2011**, *46*, 7443.
(29) Yu, H. W.; Pan, S. L.; Wu, H. P.; Han, J.; Dong, X. Y.; Zhou, Z. X. *J. Solid State Chem.* **2011**, *184*, 1644.
(30) Brown, I. D.; Altermatt, D. *Acta Crystallogr., Sect. B* **1985**, *41*, 244.
(31) Brese, N. E.; O'Keeffe, M. *Acta Crystallogr., Sect. B* **1991**, *47*, 192.
(32) Zhao, W. W.; Pan, S. L.; Han, J.; Yao, J. Y.; Yang, Y.; Li, J. J.; Zhang, M.; Zhang, L. H.; Hang, Y. *J. Solid State Chem.* **2011**, *184*, 2849.
(33) Zhang, M.; Pan, S. L.; Han, J.; Yang, Y.; Cui, L.; Zhou, Z. X. *J. Alloys Compd.* **2011**, *509*, 6696.
(34) Yu, H. W.; Pan, S. L.; Wu, H. P.; Han, J.; Li, H. Y.; Yang, Z. H. *Inorg. Chim. Acta* **2012**, *384*, 158.
(35) (a) Zhang, J. J.; Zhang, Z. H.; Sun, Y. X.; Zhang, C. Q.; Zhang, S. J.; Liu, Y.; Tao, X. T. *J. Mater. Chem.* **2012**, *22*, 9921. (b) Ok, K. M.; Halasyamani, P. S. *Inorg. Chem.* **2005**, *44*, 3919. (c) Izumi, H. K.; Kirsch, J. E.; Stern, C. L.; Poeppelmeier, K. R. *Inorg. Chem.* **2005**, *44*, 884. (d) Maggard, P. A.; Nault, T. S.; Stern, C. L.; Poeppelmeier, K. R. *J. Solid State Chem.* **2003**, *175*, 27.
(36) Lee, M. H.; Yang, C. H.; Jan, J. H. *Phys. Rev. B* **2004**, *70*, 235110.

dx.doi.org/10.1021/ic4002779 | *Inorg. Chem.* 2013, 52, 5359−5365